Effects of interface spin-orbit coupling on tunneling between normal metal and chiral *p*-wave superconductor

S. Wu and K. V. Samokhin
Department of Physics, Brock University, St. Catharines, Ontario, Canada L2S 3A1
(Received 4 May 2010; published 4 June 2010)

We study the tunneling conductance of a clean normal metal/chiral *p*-wave superconductor junction using the extended Blonder-Tinkham-Klapwijk formalism. It is shown that the spin-orbit coupling of the Rashba type that is present near the interface causes the subgap conductance peaks associated with the Andreev surface bound states to shift to a nonzero bias. We also investigate the effect of the Fermi wave vector mismatch between the normal metal and the superconductor.

DOI: 10.1103/PhysRevB.81.214506 PACS number(s): 74.55.+v, 74.45.+c, 74.20.Rp

I. INTRODUCTION

Tunneling spectroscopy is one of the most powerful probes of the electronic states in superconductors. Quasiparticles in anisotropically paired superconductors can experience a variation, e.g., a sign change, in the order parameter upon reflection from an interface. Then the interference between the incident and reflected quasiparticles results in the formation of bound states near the interface, with the energies inside the bulk energy gap, which are known as the Andreev bound states (ABS), see Refs. 1 and 2 and also a review in Ref. 3. The ABS manifest themselves in low-energy features, typically peaks, in the tunneling conductance, which have been observed experimentally. In particular, the zero-bias conductance peaks in high-T_c cuprates exhibit strong dependence on the crystallographic orientation of the interface, consistent with the *d*-wave pairing, see Ref. 4 for a review. The observation of broad subgap peaks in the tunneling conductance of Sr_2RuO_4 (Ref. 5) can also be explained in terms of the surface ABS, which are expected to exist in a chiral *p*-wave superconductor.[6,7] Other systems studied recently include the interfaces between magnetic or nonmagnetic normal metals and noncentrosymmetric or magnetic superconductors.[8–11] We would like also to mention that the zero-bias conductance peaks can originate from the quasiparticle states localized near strong impurities or surface inhomogeneities.[12] Those can be distinguished from the ABS by their different response on a magnetic field.[13]

Due to the breaking of reflection symmetry near the interface, quasiparticles experience the spin-orbit coupling (SOC) of the Rashba type,[14] even if both the normal and superconducting crystals have inversion symmetry in the bulk. The effects of such interface SOC have been neglected in the previous studies of the tunneling conductance. In this paper we focus on the properties of a junction between a normal metal and a chiral *p*-wave superconductor. It is known that the ABS in this case correspond to Majorana fermions with linear dispersion, see Refs. 7, 15, and 16. There are strong experimental indications that the chiral *p*-wave state is realized in Sr_2RuO_4 (Ref. 17). We neglect disorder and calculate the tunneling conductance using the Blonder-Tinkham-Klapwijk (BTK) formalism.[18] The effect of the Rashba SOC on the conductance can be attributed to a modification of the boundary conditions for the wave functions at the interface. We also take into account the difference between the Fermi wave vectors on the normal and superconducting sides.

The paper is organized as follows: in Sec. II, we develop a theoretical model of the normal metal-superconductor (N-S) junction with the interface SOC and use the BTK approach to calculate the amplitudes for various quasiparticle scattering processes. In Sec. III, the effects of both the interface SOC and the Fermi wave vector mismatch (FWM) on the tunneling conductance are presented and discussed. Section IV contains a summary of our results. In the Appendix, we analyze the ABS spectrum in a half-infinite chiral *p*-wave superconductor with an arbitrary interface potential. Throughout the paper we use the units in which $\hbar=1$.

II. FORMULATION OF THE MODEL

We consider a two-dimensional (2D) clean N-S junction shown in Fig. 1. The interface, which is located at $x=0$, breaks the reflection symmetry due to the crystal structure difference between the normal and superconducting sides. This leads to an asymmetric (Rashba) SOC, which is localized near the interface. The interface potential can be modeled by the following expression:

$$U(x)=[U_0+U_1\boldsymbol{n}\cdot(\hat{\boldsymbol{\sigma}}\times\hat{\boldsymbol{k}})]\delta(x), \tag{1}$$

where $\boldsymbol{n}\equiv\hat{\boldsymbol{x}}$ is the unit vector along the interface normal, U_0 and U_1 are the strengths of the spin-independent and the Rashba SOC contributions, respectively, $\hat{\boldsymbol{\sigma}}$ are the Pauli matrices, and $\hat{\boldsymbol{k}}=-i\boldsymbol{\nabla}$. The band dispersions are assumed to be parabolic, with the same effective masses of quasiparticles on both sides (according to Ref. 19, the effect of the mass difference is equivalent to that caused by a variation in the interface potential strength). On the superconducting side of the junction, we assume a chiral *p*-wave pairing state of the form $\boldsymbol{d}(\boldsymbol{k})\propto\hat{\boldsymbol{z}}(k_x+ik_y)$.

The Bogoliubov-de Gennes (BdG) equations for the four components of the quasiparticle wave function are decoupled into two independent pairs of two-component equations as follows:

$$\mathcal{H}_\sigma\Psi(\boldsymbol{r})=E\Psi(\boldsymbol{r}), \tag{2}$$

where $\sigma=\pm$ for different spin orientations,

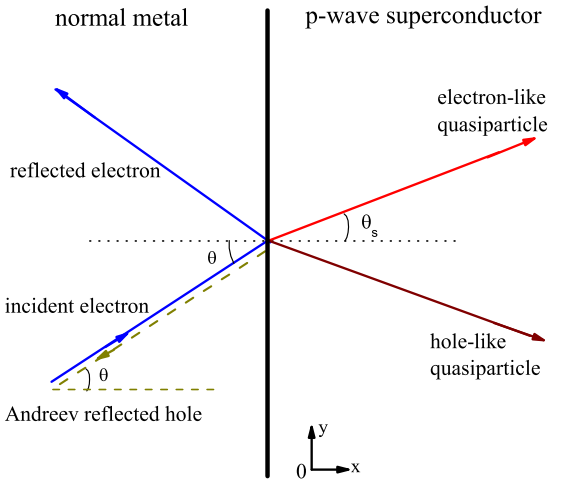

FIG. 1. (Color online) Schematic illustration of the quasiparticle reflection and transmission processes at the N-S interface.

$$\mathcal{H}_\sigma = \begin{pmatrix} -\frac{\boldsymbol{\nabla}^2}{2m} - E_{Fi} + U_\sigma(x) & \Delta(\hat{\boldsymbol{k}},\boldsymbol{r}) \\ \Delta^\dagger(\hat{\boldsymbol{k}},\boldsymbol{r}) & \frac{\boldsymbol{\nabla}^2}{2m} + E_{Fi} - U_\sigma(x) \end{pmatrix} \tag{3}$$

and $U_\sigma(x)=(U_0+i\sigma U_1\nabla_y)\delta(x)$. The Fermi energies in the normal and superconducting regions can be different due to different carrier densities, with $E_{Fi}=E_{FN}$ or E_{FS}. The ratio of the corresponding wave vectors is characterized the dimensionless FWM parameter as follows: $\lambda_0=k_{FS}/k_{FN}=\sqrt{E_{FS}/E_{FM}}$.

The off-diagonal elements of Eq. (3) contain the gap function Δ. In the spirit of the BTK approach, we neglect self-consistency and assume the gap magnitude to be equal to Δ_0 on the superconducting side and zero on the normal side. Then we have $\Delta(\hat{\boldsymbol{k}},\boldsymbol{r})=(\Delta_0/2k_{FS})\{(-i\nabla_x+\nabla_y),\theta(x)\}$, where $\theta(x)$ is the step function. The anticommutator on the right-hand side is required since the order parameter varies in space, see Ref. 16. Below we use a simpler expression: $\hat{\Delta}=(\Delta_0/k_{FS})(-i\nabla_x+\nabla_y)$, at $x>0$, neglecting the δ-function term in the off-diagonal elements, which gives a small correction to the boundary conditions.

Suppose an electron is injected from the normal metal with the excitation energy $E\geq 0$ and spin σ at an angle θ from the interface normal. The momentum parallel to the interface is conserved,

$$k_{FN}\sin\theta = k_{FS}\sin\theta_s. \tag{4}$$

The incident electron is reflected back either as an electron (normal reflection) or as a hole (Andreev reflection).[20] In the superconductor, the wave functions of the transmitted quasiparticles have both electron and hole components.

Solution of Eq. (2) has the form $\Psi(\boldsymbol{r})=e^{ik_y y}\Psi(x)$, where

$$\Psi_N(x) = \begin{pmatrix} 1 \\ 0 \end{pmatrix} e^{ik_{FN}\cos\theta x} + a_\sigma \begin{pmatrix} 0 \\ 1 \end{pmatrix} e^{ik_{FN}\cos\theta x} + b_\sigma \begin{pmatrix} 1 \\ 0 \end{pmatrix} e^{-ik_{FN}\cos\theta x} \tag{5}$$

on the normal side and

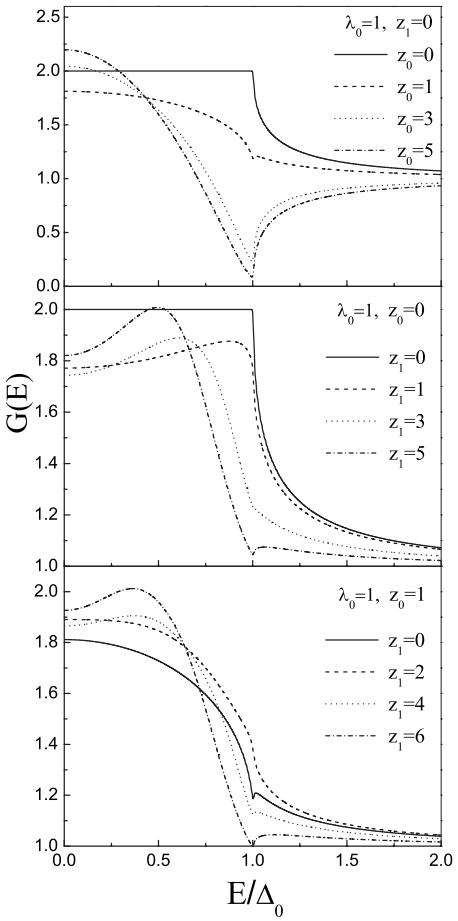

FIG. 2. The dimensionless tunneling conductance $G(E)$ versus E/Δ_0 for $\lambda_0=1$ (no FWM) and different values of Z_0 and Z_1: $Z_1=0$ (top panel), $Z_0=0$ (middle panel), and $Z_0=1$ (bottom panel).

$$\Psi_S(x) = c_\sigma \begin{pmatrix} u \\ ve^{-i\theta_s} \end{pmatrix} e^{ik_{FS}\cos\theta_s x} + d_\sigma \begin{pmatrix} -ve^{-i\theta_s} \\ u \end{pmatrix} e^{-ik_{FS}\cos\theta_s x} \tag{6}$$

on the superconducting side. Here a_σ and b_σ are the amplitudes of the Andreev and normal reflection, respectively, and c_σ and d_σ are the transmission amplitudes. The electron and hole components of the wave functions in the superconducting region are given by

$$u = \frac{1}{\sqrt{2}}\sqrt{1+\frac{\Omega}{E}}, \quad v = \frac{1}{\sqrt{2}}\sqrt{1-\frac{\Omega}{E}}, \tag{7}$$

where $\Omega=\sqrt{E^2-\Delta_0^2}$.

All the reflection and transmission amplitudes in Eqs. (5) and (6) can be found from the boundary conditions that follow from Eq. (1),

$$\Psi_S(0^+) = \Psi_N(0^-),$$

$$\Psi_S'(0^+) - \Psi_N'(0^-) = 2m(U_0 - \sigma U_1 k_{FN}\sin\theta)\Psi_N(0^-). \tag{8}$$

In particular, for the reflection amplitudes we obtain

$$a_\sigma(E,\theta) = \frac{4\lambda\omega_0 e^{-i\theta_s}}{(1+\lambda^2+Z_\sigma^2)\omega_+ + 2\lambda\omega_-},$$

$$b_\sigma(E,\theta) = \frac{[(1-iZ_\sigma)^2-\lambda^2]\omega_+}{(1+\lambda^2+Z_\sigma^2)\omega_+ + 2\lambda\omega_-}, \tag{9}$$

where

$$\lambda = \lambda_0 \frac{\cos\theta_s}{\cos\theta},$$

$$\omega_0 = \frac{u}{v}, \quad \omega_+ = \omega_0^2 + e^{-2i\theta_s}, \quad \omega_- = \omega_0^2 - e^{-2i\theta_s},$$

$$Z_\sigma = \frac{Z_0}{\cos\theta} - \sigma Z_1 \frac{\sin\theta}{\cos\theta}, \quad Z_0 = \frac{2mU_0}{k_{FN}}, \quad Z_1 = 2mU_1.$$

The dimensionless parameters Z_0 and Z_1 characterize the strengths of the potential and the Rashba SO scattering, respectively.

From the conservation of the probability current it follows that

$$|a_\sigma|^2 + |b_\sigma|^2 + \lambda(|c_\sigma|^2 + |d_\sigma|^2) = 1.$$

We note that the charge transmission at subgap energies is enhanced when the normal reflection is minimized, i.e., at $b_\sigma = 0$, which happens if $\omega_+ = 0$. Then Eq. (9) yields a subgap resonance with the energy $E = \Delta_0 \sin\theta_s$, $\theta_s > 0$, corresponding to a branch of excitations localized near the interface. This result agrees with that of Refs. 7, 15, and 16, see also the Appendix.

By using the BTK formalism,[18] we obtain for the dimensionless angle-resolved differential tunneling conductance,

$$G_\sigma(E,\theta) = 1 + |a_\sigma(E,\theta)|^2 - |b_\sigma(E,\theta)|^2$$

$$= \frac{4\lambda\{[(1+\lambda)^2+Z_\sigma^2]\omega_0^4 + 4\lambda\omega_0^2 - [(1-\lambda)^2+Z_\sigma^2]\}}{[(1+\lambda)^2+Z_\sigma^2]^2\omega_0^4 + 2\cos 2\theta[(1+\lambda)^2+Z_\sigma^2][(1-\lambda)^2+Z_\sigma^2]\omega_0^2 + [(1-\lambda)^2+Z_\sigma^2]^2}. \tag{10}$$

One can see that, although the conductance depends on the incident spin orientation: $G_+(E,\theta) \neq G_-(E,\theta)$, the time-reversal invariance is respected: $G_\sigma(E,\theta) = G_{-\sigma}(E,-\theta)$. The experimentally measurable tunneling conductance $G(E)$ is obtained after the angular integration and the summation over the incident spin orientations as follows:

$$G(E) = \frac{1}{G_N}\sum_\sigma \int_{-\pi/2}^{\pi/2} d\theta \cos\theta G_\sigma(E,\theta). \tag{11}$$

Here G_N is the conductance for a normal metal/normal metal junction with the interface potential given by Eq. (1),

$$G_N = \sum_\sigma \int_{-\pi/2}^{\pi/2} d\theta \cos\theta G_{N\sigma}(E,\theta) \tag{12}$$

with

$$G_{N\sigma}(E,\theta) = \frac{4}{4+Z_\sigma^2}. \tag{13}$$

We note that the difference between the Fermi wave vectors imposes a constraint on the effective range of angles contributing to the integrals in Eqs. (11) and (12): if $k_{FS} < k_{FN}$, then there is no transmission for $|\sin\theta| > \lambda_0$.

III. RESULTS

The tunneling conductance of the N-S junction at zero temperature can be plotted as a function of the dimensionless excitation energy E/Δ_0. We will study the effects of the interface Rashba SOC and the difference between the Fermi wave vectors on the tunneling spectra.

Let us first consider the case in which there is no FWM, i.e., $k_{FN} = k_{FS}$ and $\lambda_0 = 1$. Figure 2 shows the tunneling conductance $G(E)$ for different relative strengths of the purely potential and the SOC contributions to the interface scattering. In the top panel, we show $G(E)$ in the absence of the interface SOC ($Z_1 = 0$). The middle and bottom panels demonstrate the effects of varying the interface SOC at $Z_0 = 0$ (high-transparency barrier) and $Z_0 = 1$ (low-transparency barrier). Note that if $Z_0 = Z_1 = 0$, then $G(E) = 2$ for all subgap energies, $E < \Delta_0$, due to the Andreev reflection occurring with the probability one.

The broad peak at the subgap energies, which is most pronounced for a low-transparency interface, is associated with the surface ABS that exist in chiral p-wave superconductors[7] (we recall that there are no subgap surface bound states in s-wave superconductors and the tunneling conductance at $E < |\Delta|$ is strongly suppressed for large Z_0, Ref. 18). When we include the interface SOC, the conductance peak is shifted to a nonzero bias, see the bottom panel of Fig. 2. The origin of this effect can be attributed to a nonmonotonic angular dependence of the transmission coefficients at $Z_1 \neq 0$, which is evident from Eq. (13). Note that the spectrum of the surface ABS is not affected by the interface SOC, see the Appendix.

Next, we discuss the effect of the FWM on the tunneling conductance in two cases: (i) $\lambda_0 = 1.2$ and (ii) $\lambda_0 = 0.7$. In each

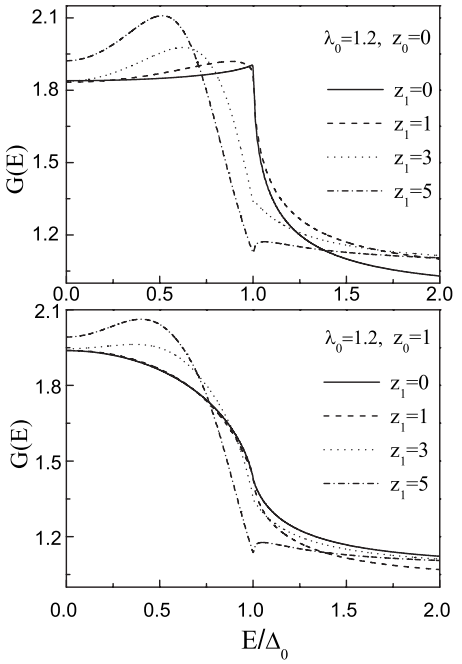

FIG. 3. The dimensionless tunneling conductance $G(E)$ versus E/Δ_0 for the FWM parameter $\lambda_0=1.2$ and different values of the interface SOC. In the top panel $Z_0=0$ (no potential barrier) and in the bottom panel $Z_0=1$ (strong potential barrier).

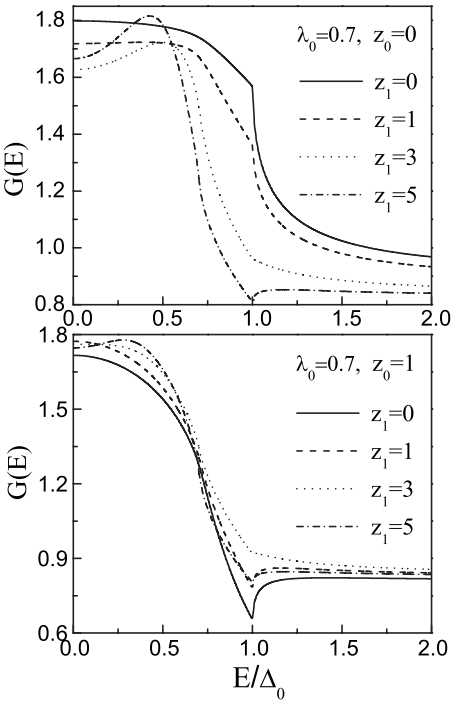

FIG. 4. The dimensionless tunneling conductance $G(E)$ versus E/Δ_0 for the FWM parameter $\lambda_0=0.7$. Other parameter values are the same as in Fig. 3.

case, we consider both high- and low-transparency interfaces, $Z_0=0$ and $Z_0=1$. Figures 3 and 4 show the variation in $G(E)$ for several values of Z_1. In the case (ii) (and for $k_{FS}<k_{FN}$, in general), the conductance is notably suppressed by the FWM because the modes with $|\sin\theta|>\lambda_0$ experience total reflection and, therefore, do not contribute to the conductance. In contrast, there is no discernible consistent effect of the FWM in the case (i).

IV. SUMMARY

In summary, we have applied the extended BTK formalism to investigate the tunneling conductance of a junction between a normal metal and a chiral p-wave superconductor. We focused on the effects of the interface SOC of the Rashba type, both with and without the Fermi-surface mismatch between the two sides of the junction. The structure of the subgap peaks in the conductance has been shown to strongly depend on the interface SOC. In particular, for a low-transparency interface, the maximum of the conductance associated with the surface ABS is shifted away from the zero bias. We also considered the case of different Fermi wave vectors in the normal and superconducting regions. When $k_{FS}<k_{FN}$, the tunneling conductance is strongly suppressed.

ACKNOWLEDGMENT

This work was supported by a Discovery Grant from the Natural Sciences and Engineering Research Council of Canada.

APPENDIX: SURFACE ABS WITH SPIN-ORBIT COUPLING

Let us consider a superconductor with a flat surface, occupying the $x\geq 0$ half space. We assume a hard-wall confining potential $V(x)$, which is infinite at $x<0$ and varies within a thin surface layer, whose thickness a is on the order of several lattice spacings. This potential results in the SOC of the form $(1/4m^2c^2)V'(x)(\hat{\boldsymbol{p}}\times\hat{\boldsymbol{\sigma}})_x$, which is also restricted to the vicinity of the surface (recall that $\hbar=1$ in our units). Assuming a 2D geometry with the band dispersion $\xi(\boldsymbol{k})$ (which includes the chemical potential), the quasiparticle spectrum can be found from the following 4×4 BdG Hamiltonian:

$$\mathcal{H}=\begin{pmatrix}\hat{\epsilon} & \hat{\Delta}\\ \hat{\Delta}^{\dagger} & -\hat{\epsilon}^{T}\end{pmatrix}, \tag{A1}$$

where $\hat{\epsilon}=\xi(-i\boldsymbol{\nabla})+V(x)-(i/4m^2c^2)V'(x)\hat{\sigma}_3\nabla_y$ is the single-particle Hamiltonian. In a triplet pairing state, the order parameter is given by $\hat{\Delta}=(i\hat{\boldsymbol{\sigma}}\hat{\sigma}_2)\boldsymbol{d}(\hat{\boldsymbol{k}},\boldsymbol{r})$. To make analytical progress, we neglect self-consistency and assume that the order parameter is uniform at all $x>a$. The system is translationally invariant along the surface and the wave functions have the form $\Psi(\boldsymbol{r})=e^{ik_y y}\Psi(x)$.

For a chiral p-wave state of the form $\boldsymbol{d}\propto\hat{\boldsymbol{z}}(k_x+ik_y)$, it is easy to show that Eq. (A1) can be written as a direct sum of two 2×2 Hamiltonians given by

$$\mathcal{H}_\sigma = \begin{pmatrix} \hat{\xi} + U_\sigma(x) & \hat{\Delta} \\ \hat{\Delta}^\dagger & -\hat{\xi} - U_\sigma(x) \end{pmatrix}, \tag{A2}$$

where $\sigma = \pm$, $U_\sigma(x) = V(x) - \sigma(1/4m^2c^2)V'(x)k_y$, and the gap function is given by $\hat{\Delta} = (\Delta_0/k_F)(-i\nabla_x + ik_y)$, with $k_F \equiv k_{FS}$ being the Fermi wave vector.

In the region $x > a$, $U_\sigma(x) = 0$, and the spectra of $\mathcal{H}_\sigma$ can be analyzed in the semiclassical, or Andreev, approximation.[20] We represent wave functions in the form $\Psi(x) = e^{ik_x x}\psi(x)$, where k_x satisfies the equation

$$\xi(k_x, k_y) = 0 \tag{A3}$$

at fixed k_y. Each Fermi-surface wave vector $\boldsymbol{k} = (k_x, k_y)$ defines a semiclassical trajectory, along which the quasiparticle state is described by a coherent superposition of the electron and hole amplitudes: $\psi(x) = [\psi_e(x), \psi_h(x)]^T$, satisfying the Andreev equation,

$$\begin{pmatrix} -iv_{F,x}(\boldsymbol{k})\nabla_x & \Delta(\boldsymbol{k}) \\ \Delta^*(\boldsymbol{k}) & iv_{F,x}(\boldsymbol{k})\nabla_x \end{pmatrix} \psi(x) = E\psi(x), \tag{A4}$$

where $\boldsymbol{v}_F(\boldsymbol{k}) = \partial\xi/\partial\boldsymbol{k}$ is the quasiparticle velocity on the Fermi surface, $E \geq 0$ is the energy of excitations, and

$$\Delta(\boldsymbol{k}) = \Delta_0 \frac{k_x + ik_y}{k_F}. \tag{A5}$$

Depending on the direction of propagation, the semiclassical trajectories are classified as either incident ($v_{F,x} < 0$) or reflected ($v_{F,x} > 0$).

One can seek solution of Eq. (A4) in the form of a plane wave: $\psi(x) \sim e^{iqx}$. Focusing on the quasiparticle states which are bound to the surface, but cannot exist in the bulk, we expect that $E \leq \Delta_0$. For the wave function we then obtain:

$$\psi_{\boldsymbol{k}}(x) = \frac{1}{\sqrt{2}} \begin{pmatrix} 1 \\ \alpha(\boldsymbol{k}) \end{pmatrix} e^{-\kappa(\boldsymbol{k})x}, \tag{A6}$$

where

$$\alpha(\boldsymbol{k}) = \frac{\Delta^*(\boldsymbol{k})}{E + i\Omega(\boldsymbol{k})\,\mathrm{sign}\, v_{F,x}(\boldsymbol{k})}, \quad \kappa(\boldsymbol{k}) = \frac{\Omega(\boldsymbol{k})}{|v_{F,x}(\boldsymbol{k})|},$$

and $\Omega(\boldsymbol{k}) = \sqrt{|\Delta(\boldsymbol{k})|^2 - E^2} = \sqrt{\Delta_0^2 - E^2}$.

The Andreev approximation is not valid near the surface, at $0 < x < a$, where the rapidly varying potential $U_\sigma(x)$ is nonzero. The surface scattering will result in the effective boundary conditions at $x = a$, which express the Andreev wave functions corresponding to the reflected trajectories in terms of those corresponding to the incident trajectories.[21]

Depending on the band structure and the surface orientation, Eq. (A3) might have several solutions. In the case of a parabolic band, there is only one incident and one reflected trajectory at each k_y (except $k_y = \pm k_{FS}$, where the Andreev approximation is not applicable): $\boldsymbol{k}_{in} = (-k_x, k_y)$, $\boldsymbol{k}_{out} = (k_x, k_y)$, with $k_x > 0$. The effective boundary condition has the following form:

$$\psi_{\boldsymbol{k}_{out}}(a) = \hat{S}\psi_{\boldsymbol{k}_{in}}(a), \tag{A7}$$

where $\hat{S}$ is the surface scattering matrix, which is an electron-hole scalar[21] determined by the surface potential $U_\sigma(x)$. Inserting here the wave functions [Eq. (A6)], we arrive at an equation for the bound-state energy,

$$\frac{E + i\Omega(\boldsymbol{k}_{in})}{E - i\Omega(\boldsymbol{k}_{out})} = \frac{\Delta(\boldsymbol{k}_{in})}{\Delta(\boldsymbol{k}_{out})}. \tag{A8}$$

For the chiral p-wave state [Eq. (A5)], the solution is given by

$$E(k_y) = \Delta_0 \frac{k_y}{k_F} \quad (k_y > 0). \tag{A9}$$

Remarkably, this expression does not contain any microscopic details (in particular, it has the same form for $\mathcal{H}_+$ and $\mathcal{H}_-$), which is consistent with a topological nature of the surface ABS.[22] We come to the conclusion that the surface bound states of Hamiltonian (A1) are described by two ($\sigma = \pm$) degenerate branches of fermionic excitations with linear dispersion, given by Eq. (A9), regardless of the SOC strength.

[1] C. R. Hu, Phys. Rev. Lett. **72**, 1526 (1994).
[2] S. Kashiwaya, Y. Tanaka, M. Koyanagi, H. Takashima, and K. Kajimura, Phys. Rev. B **51**, 1350 (1995).
[3] S. Kashiwaya and Y. Tanaka, Rep. Prog. Phys. **63**, 1641 (2000).
[4] T. Löfwander, V. S. Shumeiko, and G. Wendin, Supercond. Sci. Technol. **14**, R53 (2001).
[5] Z. Q. Mao, K. D. Nelson, R. Jin, Y. Liu, and Y. Maeno, Phys. Rev. Lett. **87**, 037003 (2001).
[6] M. Yamashiro, Y. Tanaka, and S. Kashiwaya, Phys. Rev. B **56**, 7847 (1997).
[7] C. Honerkamp and M. Sigrist, J. Low Temp. Phys. **111**, 895 (1998).
[8] T. Yokoyama and Y. Tanaka, Phys. Rev. B **75**, 132503 (2007).
[9] C. Iniotakis, N. Hayashi, Y. Sawa, T. Yokoyama, U. May, Y. Tanaka, and M. Sigrist, Phys. Rev. B **76**, 012501 (2007).
[10] J. Linder and A. Sudbø, Phys. Rev. B **76**, 054511 (2007).
[11] S. Wu and K. V. Samokhin, Phys. Rev. B **80**, 014516 (2009).
[12] A. V. Balatsky, I. Vekhter, and J.-X. Zhu, Rev. Mod. Phys. **78**, 373 (2006).
[13] K. V. Samokhin and M. B. Walker, Phys. Rev. B **64**, 172506 (2001).
[14] E. I. Rashba, Fiz. Tverd. Tela (Leningrad) **2**, 1224 (1960) [Sov. Phys. Solid State **2**, 1109 (1960)].
[15] N. Read and D. Green, Phys. Rev. B **61**, 10267 (2000).
[16] M. Stone and R. Roy, Phys. Rev. B **69**, 184511 (2004).
[17] A. P. Mackenzie and Y. Maeno, Rev. Mod. Phys. **75**, 657 (2003).
[18] G. E. Blonder, M. Tinkham, and T. M. Klapwijk, Phys. Rev. B **25**, 4515 (1982).
[19] T. Yokoyama, Y. Tanaka, and J. Inoue, Phys. Rev. B **74**, 035318 (2006).

[20] A. F. Andreev, Zh. Eksp. Teor. Fiz. **46**, 1823 (1964) [Sov. Phys. JETP **19**, 1228 (1964)].

[21] A. L. Shelankov, Pis'ma Zh. Eksp. Teor. Fiz. **32**, 122 (1980) [JETP Lett. **32**, 111 (1980)]; A. Millis, D. Rainer, and J. A. Sauls, Phys. Rev. B **38**, 4504 (1988); A. Shelankov and M. Ozana, *ibid.* **61**, 7077 (2000).

[22] G. E. Volovik, Pis'ma Zh. Eksp. Teor. Fiz. **66**, 492 (1997) [JETP Lett. **66**, 522 (1997)].